Cement and Concrete Research 40 (2010) 189–196

Contents lists available at ScienceDirect

Cement and Concrete Research

journal homepage: http://ees.elsevier.com/CEMCON/default.asp

The evolution of strength and crystalline phases for alkali-activated ground blast furnace slag and fly ash-based geopolymers

Jae Eun Oh [a], Paulo J.M. Monteiro [a,*], Ssang Sun Jun [b], Sejin Choi [a], Simon M. Clark [c,d]

[a] Department of Civil and Environmental Engineering, University of California, Berkeley, CA 94720, USA
[b] Global Leading Offshore Plant Education Center, Korea Maritime University, Busan, 606-791, Republic of Korea
[c] Advanced Light Source, Lawrence Berkeley National Laboratory, Berkeley, CA 20015, USA
[d] Department of Earth and Planetary Sciences, University of California, Berkeley, CA 94720, USA

ARTICLE INFO

Article history:
Received 6 February 2009
Accepted 6 October 2009

Keywords:
Alkali-activated cement (D)
Geopolymer (D)
X-ray diffraction (B)
Fly ash (D)
Granulated blast furnace slag (D)

ABSTRACT

The increase in strength and evolution of crystalline phases in inorganic polymer cement, made by the alkali activation of slag, Class C and Class F fly ashes, was followed using compressive strength test and synchrotron X-ray diffraction. In order to increase the crystallinity of the product the reactions were carried out at 80 °C. We found that hydrotalcite formed in both the alkali-activated slag cements and the fly ash-based geopolymers. Hydroxycancrinite, one member of the ABC-6 family of zeolites, was found only in the fly ash geopolymers. Assuming that the predominantly amorphous geopolymer formed under ambient conditions relates to the crystalline phases found when the mixture is cured at high temperature, we propose that the structure of this zeolitic precursor formed in Na-based high alkaline environment can be regarded as a disordered form of the basic building unit of the ABC-6 group of zeolites which includes poly-types such as hydroxycancrinite, hydroxysodalite and chabazite-Na.

1. Introduction

Alkali activation of industrial aluminosilicate waste materials, such as fly ash or ground blast furnace slag, produces high strength binder under highly alkaline conditions (pH = 12–14.5). This binder has great potential as an environmentally favorable alternative to portland cement. It could produce a binder with the advantages of portland cement but at a lower cost, with a large reduction in CO_2 emissions and will recycle an industrial waste material as a raw material. Examples of this type of binder include Class F fly ash (low calcium fly ash) based geopolymer (FFG) [1–3] and alkali-activated slag cement (AAS) [4–8].

The synthesis conditions for AAS and FFG are quite similar but their reaction products are quite different [1,2]. The major chemical product for FFG is amorphous hydrated alkali-aluminosilicate [1–3] while for AAS it is C-S-H (I) [4–8]. The major difference between the two products is that calcium is not necessary in forming geopolymer product. From a chemical composition point of view in terms of CaO and SiO_2 content, Class C fly ash (high calcium fly ash) is somewhere between Class F fly ash and granulated blast furnace slag (SLAG). Other components, such as Al_2O_3, are much the same. It may be expected that a binder produced by alkali activation of Class C fly ash (FCG) may have shared features found in both AAS and FFG [9].

The addition of alkali-silicate solution (e.g. waterglass, Na_2SiO_3 or K_2SiO_3) can raise the rate of strength development as well as largely enhance the final strength by promoting the hydrolysis of the siliceous and aluminum species of the raw materials as well as providing additional silicate species, sodium, or potassium ions, which alkaline ions are required for geopolymerization [2,3,10]. The effect of adding the waterglass to the reaction mixture on the final phases present in the reaction product has not yet been cleared.

Many studies have concluded that geopolymer binder may be viewed as an amorphous analogue of zeolites or zeolitic precursors [1,11,12]. The analogue of hydrothermal zeolite synthesis [13–16] to geopolymerization has been proposed based on similarities such as raw materials and activating solutions [2,11] However, geopolymerization uses a relatively lower solution/binder ratio, less than 0.6, and lower reaction temperature, under 90 °C. This leads to the geopolymer products being nearly amorphous [1–3].

Geopolymer binder is generally synthesized in a temperature range of 20–90 °C [2]. Geopolymers formed at room temperature are amorphous. With increasing temperature, crystalline phases begin to appear. However, there have not been any detailed studies of the effect of curing temperature on the properties of the geopolymer.

Here we use synchrotron X-ray diffraction (XRD), mechanical strength testing and scanning electron microscopy (SEM) to explore the similarities and differences between AAS, FFG and FCG formed at 80 °C. We also present some data where the alkali activating solution has been buffered with sodium silicate solution (waterglass) before activating fly ash C.

* Corresponding author.
E-mail address: monteiro@berkeley.edu (P.J.M. Monteiro).

0008-8846/$ – see front matter © 2009 Elsevier Ltd. All rights reserved.
doi:10.1016/j.cemconres.2009.10.010

2. Experimental program

Ground granulated blast furnace slag (SLAG) was obtained from Independent Cement & Lime Pty. Ltd., Australia. Class C fly ash (FAC) and Class F fly ash (FAF) were obtained from the Bridger plant (Northern California) of Headwaters Resources. The chemical compositions of the raw materials were determined using a Phillips PW2400 wavelength-dispersive X-ray fluorescence (XRF) spectrometer and are given in Table 1. These materials were activated with the following activators: (1) 10 M analytical grade NaOH solution (Fisher Scientific, S318-1 sodium hydroxide, Certified ACS pellets) to synthesize samples FAC_N, FAF_N and SLAG_N; (2) waterglass [from PQ Corporation, N®38 sodium silicate solution, weight ratio $SiO_2/Na_2O = 3.22$, wt.%$Na_2O = 8.2$, wt.%$SiO_2 = 26.4$, wt.%$H_2O = 65.4$, pH = 11.02 (measured value)] to give samples FAF_W0.4, FAF_W1.0, FAC_W and SLAG_W; (3) a mixture of these two solutions to produce sample FAC_NW. Full details of these mixtures are contained in Table 2. We attempted to set the solution to binder (s/b) values to 0.4, but this could only be partially achieved owing to the poor workability of some waterglass-only samples (e.g. FAC_W and SLAG_W); for these cases the s/b was increased to give a suitable workability. The s/b of FAF_W1.0 was chosen to test the effect of higher s/b ratio. Samples were reacted in cylinder molds measuring ϕ2.54 cm × 2.54 cm. All samples were cured at 80 °C in a 100% relative humidity using a water bath for 2 h, 4 h, 1 day, 3 days, 7 days and 14 days. XRD samples were quenched with acetone to stop the reaction.

Scanning electron micrographs were collected using a CAMECA SX100 from gold coated exposed surfaces obtained by cutting cylindrical samples in half. Compressive strength tests were made using a Baldwin Universal testing machine. XRD patterns were collected using beamline 12.2.2 at the Advanced Light Source, Lawrence Berkeley National Laboratory [17] using a wavelength of λ = 0.4959 Å. Two dimensional diffraction patterns collected using a mar345 image plate were reduced to normal one dimensional patterns using the FIT2D program [18]. Peak positions were determined by fitting the data with pseudo-voigt profiles using the XFIT program [19].

3. Results and discussion

3.1. Scanning electron microscopy images

The scanning electron micrographs contained in Fig. 1 represent typical microstructures found in the reaction products obtained from our investigation. Comparison of the micrographs of FAC_N and FAC_W shows that a few unreacted fly ash spheres are covered with newly formed glassy crust in FAC_N paste, whereas in FAC_W paste, higher proportion of unreacted fly ash spheres remain in the matrix (see (b) in Fig. 1). On the other hand, for the other pastes (alkali-activated slag and FAF paste), microstructures of matrices do not depend on type of activator.

Table 1
Chemical composition (wt.%) of the raw materials.

Oxide	FAF	FAC	SLAG
SiO_2	62.00	45.65	33.04
Al_2O_3	18.89	17.28	13.35
Fe_2O_3	4.90	5.15	0.18
CaO	5.98	19.91	41.78
MgO	1.99	4.42	6.02
Na_2O	2.41	1.75	0.20
K_2O	1.14	0.59	0.37
TiO_2	1.09	1.36	1.15
P_2O_5	0.26	0.74	0.02
MnO	0.04	0.04	0.35
Total	98.70	98.70	96.89

FAF: Class F fly ash, FAC: Class C fly ash, SLAG: ground granulated blast furnace slag.

Table 2
Mixture proportions of samples in weight (g).

Label	Binding raw materials (g)			Activators (g)		s/b (wt./wt.)	Curing temp. (°C)
	SLAG	FAF	FAC	NaOH solution (10 M)	Waterglass (Ms = 3.22)		
FAC_N	0.0	0.0	125.0	50.0	0.0	0.40	80.0
FAF_N	0.0	125.0	0.0	50.0	0.0	0.40	80.0
SLAG_N	125.0	0.0	0.0	50.0	0.0	0.40	80.0
FAC_NW	0.0	0.0	125.0	40.0	10.0	0.40	80.0
FAF_W0.4	0.0	125.0	0.0	0.0	50.0	0.40	80.0
FAF_W1.0	0.0	125.0	0.0	0.0	125.0	1.00	80.0
FAC_W	0.0	0.0	125.0	0.0	80.0	0.64	80.0
SLAG_W	125.0	0.0	0.0	0.0	125.0	1.00	80.0

Labels indicate that FAC: Class C fly ash, FAF: Class F fly ash, N: NaOH solution, W: waterglass (= sodium silicate solution), s/b: solution to binder weight ratio. The number following the 'W' indicates the s/b for FAF_W0.4 and FAF_W1.0.

3.2. Strength development

The compressive strength development for our samples is shown in Fig. 2 and the value of the 14-day compressive strength with experimental parameters is contained in Table 3.

The pastes activated with NaOH-only solution quickly gained higher strength [FAC_N, FAF_N, SLAG_N, and FAC_NW; see (a) and (c) in Fig. 2]. Pastes activated with waterglass only showed very low strength [FAC_W and SLAG_W, see (b) in Fig. 2] or delayed strength gain [FAF_W0.4 and FAF_W1.0, see (b) in Fig. 2]. In waterglass-only samples, the major difference in chemical composition between the high strength and low strength samples is the calcium content of the raw materials. In the absence of sodium hydroxide, it was clearly observed that the use of waterglass immediately reduced the workability of Ca-rich sample paste, leading to a large reduction in the compressive strength. In the presence of sodium hydroxide, the addition of waterglass largely enhanced the compressive strength in Ca-rich fly ash pastes (compare FAC_NW and FAC_N) without causing any workability problem. Earlier measurements reported that high strength was also achieved even when only waterglass is used without alkali hydroxide for fly ash [20,21] and slag [22,23]; however, in those studies the Ms modulus (the mass ratio of SiO_2 to Na_2O) of the waterglass solution ranged from 1 to 1.5 in order to gain a high strength [21–23]; whereas, the Ms in the present study was as high as 3.22.

Besides the calcium content, there are well-known other factors affecting mechanical strength reported in the literature [2], including the molar ratio of available (Na + K) to Al in a mixture, which is required to be close to one to give balanced charges in the geopolymer structure. In this investigation, a simple comparison of (Na + K)/Al ratios between FAF_W0.4 and FAF_W1.0 seems to predict the compressive strength better than the solution to binder ratios because the compressive strength of FAF_W1.0 appeared higher than that of FAF_W0.4 (the numbers following the letter W indicate s/b).

3.3. X-ray diffraction

XRD patterns collected after curing for: 0 h, 2 h, 6 h and 14 days are shown in Fig. 3. Some new peaks are seen to appear during curing and some of the original peaks are seen to increase in intensity. The positions of these peaks are tabulated in Table 4 together with phase assignations. All patterns are seen to contain amorphous humps at around 2.0–4.0 Å.

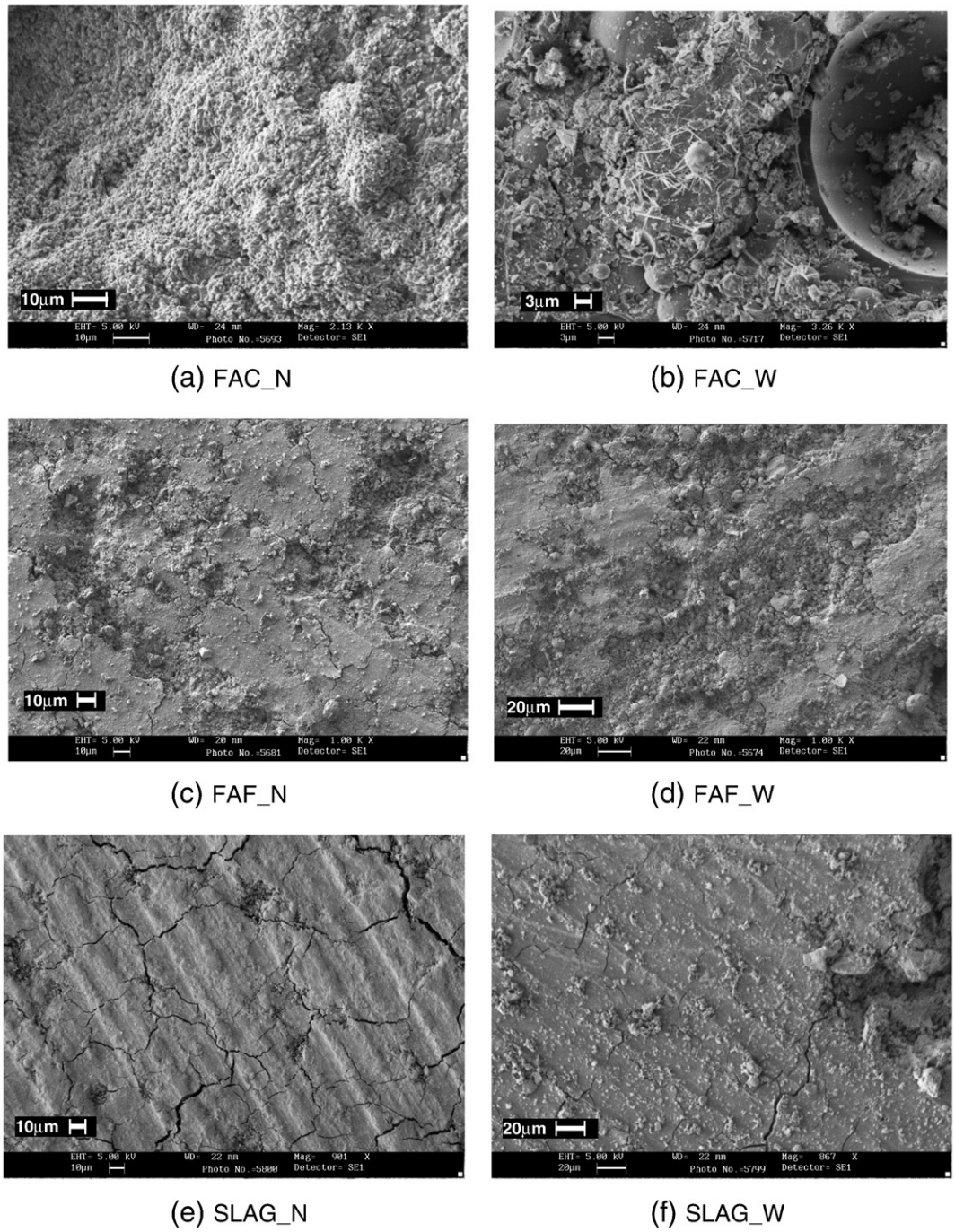

Fig. 1. SEM micrographs for 14-day cured samples.

3.3.1. Alkali activation by sodium hydroxide (SLAG_N, FAC_N, FAC_NW and FAF_N)

It is well known that hydrotalcite and C-S-H (I) are the main products of alkali-activated slag when Mg is present [5–8]. Hydrotalcite is a mineral having the formula, $Mg_6Al_2CO_3(OH)_{16}\cdot 4H_2O$ [24] and has been frequently observed in Ca-rich pastes of alkali-activated slag [5–8]. In our investigation, the hydrotalcite phase is found not only in our activated slag sample (SLAG_W) but also in all the pastes of NaOH activated fly ash geopolymers (FAC_N, FAC_NW, and FAF_N). This indicates that: (1) the formation of hydrotalcite is not unique to Ca-rich samples, that is, it is not controlled by Ca content, and (2) considering the same Al-bearing product can be produced from both SLAG and FAC or FAF, the intermediate chemical states of dissolved aluminum species may be similar.

No calcium hydroxide (portlandite) was found in the alkali-activated FAC despite its high Ca content, whereas, relatively strong calcium hydroxide peaks are identified in the alkali-activated SLAG paste, implying that the chemical form of calcium in raw materials is much different between SLAG and FAC. In order for calcium hydroxide to precipitate in high pH solution, the dissolution of Ca from the raw materials should be a prerequisite. The absence of calcium hydroxide in Class C fly ash paste, therefore, possibly indicates a low degree of dissolution of calcium in FAC. This explains why very little C-S-H (I) was formed from FAC. Less reactive calcium content in a raw material results in a lower amount of C-S-H (I) formation. Although a few C-S-H (I) peaks are observed in FAC pastes, the intensity of the C-S-H (I) peaks is very weak. Also, the long-range-ordering characteristic peak of C-S-H (I) at $d = \sim 12.5$ Å was absent in the FAC pastes. This may indicate that the

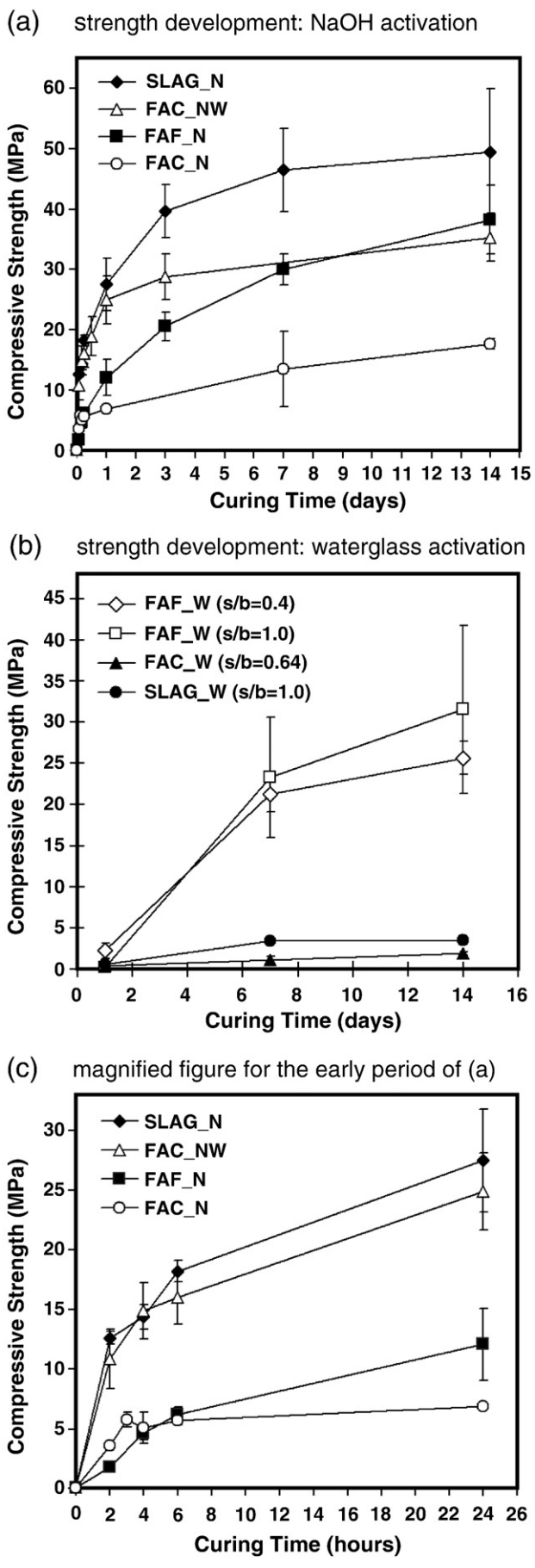

Fig. 2. Strength development of alkali-activated slag and fly ash-based geopolymers using NaOH solution and waterglass; the mechanical strength FAC with NaOH is lower than that of FAF paste possibly due to its high unreacted calcium content. Addition of waterglass (Ms = 3.22) in FAC largely increases the mechanical strength, but there was no major phase difference in the XRD patterns.

calcium in FAC is not generally involved in the formation of C-S-H (I) or geopolymer. Instead it seems to remain unreacted and may even possibly reduce the mechanical strength [compare FAC_N and FAF_N in (a) of Fig. 2 and Table 4]. Some reports have claimed that calcium content increases the mechanical strength of geopolymer [25]. However, most studies did not clearly distinguish the chemical form of the calcium. It could be Ca in the raw materials, Ca in the final reaction product, or Ca in the added $Ca(OH)_2$. From our findings, we may draw the conclusion that whether harmful or beneficial effect of calcium content largely depends on the chemical form of the calcium in the raw materials.

In all fly ash pastes activated with NaOH, many of the strong peaks are identified as being due to hydroxycancrinite ($a = 12.740$ Å, $c = 5.182$ Å, space group: P3 of hexagonal unit cell, chemical formula, $[Na_6(OH)_2][Na_2(H_2O)_2](Si_6Al_6O_{24})$) [26]. Hydroxycancrinite is a zeolite mineral [27] that belongs to the cancrinite group of zeolites [26], which belong to the ABC-6 family of zeolite crystal structures [28]. Other well-known zeolite minerals belonging to the ABC-6 family are sodalite, levyne, chabazite and offretite. The ABC-6 family is characterized by a basic structural layer consisting of six-membered rings of Al- and Si-tetrahedra as shown in (a) of Fig. 4. Only 19 members of 176 zeolite framework types can be described as ABC-6 family [28]. The main difference between zeolites belonging to the ABC-6 family is only in the stacking sequence of this basic layer. If the position of one six-membered ring on one layer is called 'A' and the two possible positions of the next layer above A are called 'B' and 'C' respectively, all the stacking sequences of the basic layers of the ABC-6 group of minerals can be described by 'AB', 'ABC' or 'AABB' and so on. Hydroxycancrinite adopts the 'ABAB' arrangement and chabazite the 'AABBCC' arrangement [26].

Different types of zeolite synthesis, including hydroxycancrinite from coal fly ash using alkaline activation, have been explored with various techniques [13–15] and summarized well by Querol [16]. The formation of hydroxycancrinite from alkali activation of blast furnace slag under hydrothermal conditions has also been reported [29]. Zeolite synthesis using fly ash can be regarded as an analogue of geopolymer production in many ways. All previous studies have utilized a similar methodology in their zeolite synthesis, which is based on; (1) the dissolution of aluminosilicate phases in Class F fly ash with alkaline solution; (2) the subsequent precipitation of zeolite. These methods are also similar to the methodology of geopolymer production except that zeolite synthesis is usually carried out in a dilute system under hydrothermal conditions at between 150 and 200 °C [11]. It should be also noted that the concentration of sodium hydroxide determines the species of zeolitic reaction products; high concentration (> 5 M) of NaOH usually generates the cancrinite group of minerals such as herschelite, hydroxysodalite or hydroxycancrinite, whereas a low concentration (0.5–3 M) of NaOH produces zeolite Na-P1, faujasite [15,16]. Considering the similar high NaOH concentration (> 5 M) used in geopolymerization, it can be expected that in case of NaOH activator, the zeolitic precursor must be similar to the ABC-6 family of zeolite minerals in the crystal structure. However, due to the limited resolution of conventional XRD instruments, it has been very difficult to determine what type of zeolitic crystallites forms in geopolymeric gel. From our findings, we may conclude that the geopolymer may simply be a disordered form of the ABC-6 family of zeolitic products having various poly-types such as chabazite, hydroxysodalite or hydroxycancrinite from amorphous structure to polycrystalline in case of high concentration (~10 M) of NaOH activator. In addition, the zeolitic precursor may be the single layer

Table 3
Experimental parameters and 14-day compressive strength of activated pastes.

Parameters	FAC_N	FAF_N	SLAG_N	FAC_NW	FAF_W0.4	FAF_W1.0	FAC_W	SLAG_W
Solution/binder (= *s*/*b*) (wt./wt.)	0.40	0.40	0.40	0.40	0.40	1.00	0.64	1.00
Water/binder (wt./wt.)	0.28	0.28	0.28	0.28	0.26	0.65	0.42	0.65
Si/Al (molar)	2.24	2.78	2.10	2.35	3.26	3.97	3.07	3.78
(Na + K)/Al (molar)	1.09	1.09	1.20	0.98	0.56	0.99	0.70	1.07
SiO_2/Al_2O_3 (molar)	4.48	5.57	4.20	4.69	6.52	7.94	6.14	7.56
Na_2O/Al_2O_3 (molar)	1.05	1.02	1.17	0.94	0.50	0.92	0.67	1.04
M_2O/SiO_2 (molar)	0.24	0.20	0.29	0.21	0.09	0.12	0.11	0.14
M_2O/Al_2O_3 (molar)	1.09	1.09	1.20	0.98	0.56	0.99	0.70	1.07
Ms (= SiO_2/Na_2O) (wt. ratio) in total alkali activator solution	0.00	0.00	0.00	0.26	3.22	3.22	3.22	3.22
wt.% of NaOH solution in total alkali activator solution	100.0	100.0	100.0	80.0	0.0	0.0	0.0	0.0
wt.% of waterglass in total alkali activator solution	0.0	0.0	0.0	20.0	100.0	100.0	100.0	100.0
pH of alkali activator solution	14.51	14.51	14.51	14.38	11.02	11.02	11.02	11.02
Compressive strength (MPa), 14-day cured samples	17.6 ± 0.9	38 ± 6	50 ± 11	35 ± 4	26 ± 2	30 ± 10	1.8 ± 0.2	3.5 ± 0.4

M: alkali metal (e.g. Na, K), binding raw materials were Class C fly ash, Class F fly ash or slag, activating solution = NaOH solution, waterglass, or a mixture of NaOH and waterglass.

of the ABC-6 family structure as shown in Fig. 4. This conclusion is supported by the earlier geopolymer studies reporting a presence of Na-chabazite, sodalite, cancrinite [10] and hydroxysodalite [20] in alkali-activated fly ash with similar synthesizing conditions.

It is not still clear if the core material creating the strength of geopolymer resembles hydroxycancrinite or hydrotalcite or another unknown amorphous species. Also, it has been reported that more amorphous geopolymer matrix formed by using waterglass in activator showed higher compressive strength [10], implying that the crystalline phases may not contribute much to the compressive strength of geopolymer. However, we should also note that higher curing temperature increases not only zeolitic crystalline phases, but also the degree of reaction and the mechanical strength of geopolymer [2,9], and that the geopolymer was found to have a nanometric size of zeolite-type three dimensional structure [12]. Therefore, it is highly probable that the crystalline zeolite phases found in geopolymers [10,20] may show us some clue of the core material, which must be a nano-crystalline or amorphous form of the ABC-6 family group of zeolite.

From earlier zeolite synthesis studies [13–16], it has been reported that the reaction products depend not only the concentration of alkali hydroxide, but also on alkali type of hydroxide solution. In the event that KOH solution was used, chabazite K, zeolite linde F or kalsilite was usually produced [13,16]; whereas, on using NaOH solution, the zeolitic products were zeolite Na-P1, analcime, hydroxysodalite or hydroxycancrinite; that is, although all reaction products are included in the zeolite group, they have different category of crystal structure. This trend may be applicable to geopolymerization regarding why mechanical properties of geopolymer depend on the alkali species of alkali hydroxide (e.g. KOH and NaOH) [30].

Besides hydrotalcite and hydroxycancrinite phases, there are some other unidentified strong peaks commonly observed in XRD diagrams. Strong peaks at $d = 4.38–4.40$ Å, 2.01–2.02 Å. and 1.72–1.73 Å phases are found in only Ca-rich samples (Class C fly ash and slag). Those peaks seem to relate with Ca-related reaction products, but not seem to consume Ca much in forming the products.

3.3.2. Alkali activation of waterglass (= sodium silicate solution)

FAC_W and SLAG_W samples showed not only very low strength but also no newly emerged XRD peaks compared with those of raw materials, whereas the samples FAF_W1.0 and FAF_W0.4 generated relatively high strength at later stage after 7 days from mixing, as well as some new created peaks. However, the XRD patterns of FAF_W1.0 and FAF_W0.4 are significantly different from those from the paste activated with NaOH. These patterns are found to be similar only to those of some members of the ABC-6 family such as franzinite (JCPDS card 30-1170), levyne (JCPDS card 11-0582), afghanite (JCPDS card 20-1086), zeolite SAPO-56 (JCPDS card 52-1178) although there is no exactly matched pattern. Although theses zeolites cannot be made from the chemical composition of the current geopolymerization, the XRD patterns indicate that the framework topology of the zeolitic precursor seem to resemble these zeolites. This can also support the zeolitic precursor of geopolymer may be the single layer of the ABC-6 family of zeolite.

Regarding the effect of waterglass on geopolymerization in the presence of NaOH, comparison of XRD patterns of FAC_N with FAC_NW reveals that there is no different peak resulting from waterglass although diffracted intensities of each peak were largely different in XRD patterns. This result implies that the addition of waterglass does not make any new phase although it largely enhances compressive strength as well as the rate of alkali activation.

4. Conclusions

We used synchrotron X-ray diffraction on slag and fly ash pastes activated with sodium hydroxide, sodium silicate or a mixture of these two solutions to explore what types of zeolitic precursors are present. SEM imaging and compressive strength tests were also performed to correlate the XRD results with microstructure and compressive strength. The results indicate that:

1. When raw materials are activated with NaOH solution with or without waterglass, major crystalline phases of activated SLAG were C-S-H (I) and hydrotalcite, but no zeolite was found. Fly ash-based samples were also found to produce hydrotalcite, which has not been previously identified in geopolymer studies. In the fly ash samples, hydroxycancrinite was identified as the major crystalline phase. Similarly, when a waterglass-only solution was used as the activator an ABC-6 family type of crystalline phase was also identified. Thus, our investigation proposes that the zeolitic precursors may be a disordered form of some of the ABC-6 family of zeolites having poly-types such as: hydroxycancrinite, hydroxysodalite, chabazite, levyne or franzinite depending on pH environment of pastes. However, we should note that this result is only valid when an activator contains mainly sodium (e.g. NaOH or sodium silicate solution). Considering earlier zeolite synthesis studies, if a potassium-based activator (e.g., KOH) is used, different types of zeolitic precursors may form.
2. Despite a high calcium content only very weak C-S-H (I) peaks and no $Ca(OH)_2$ phase were found in the FAC paste activated with NaOH solution. This implies that the Ca in FAC does not dissolve in the activator solution as readily as the Ca in SLAG.

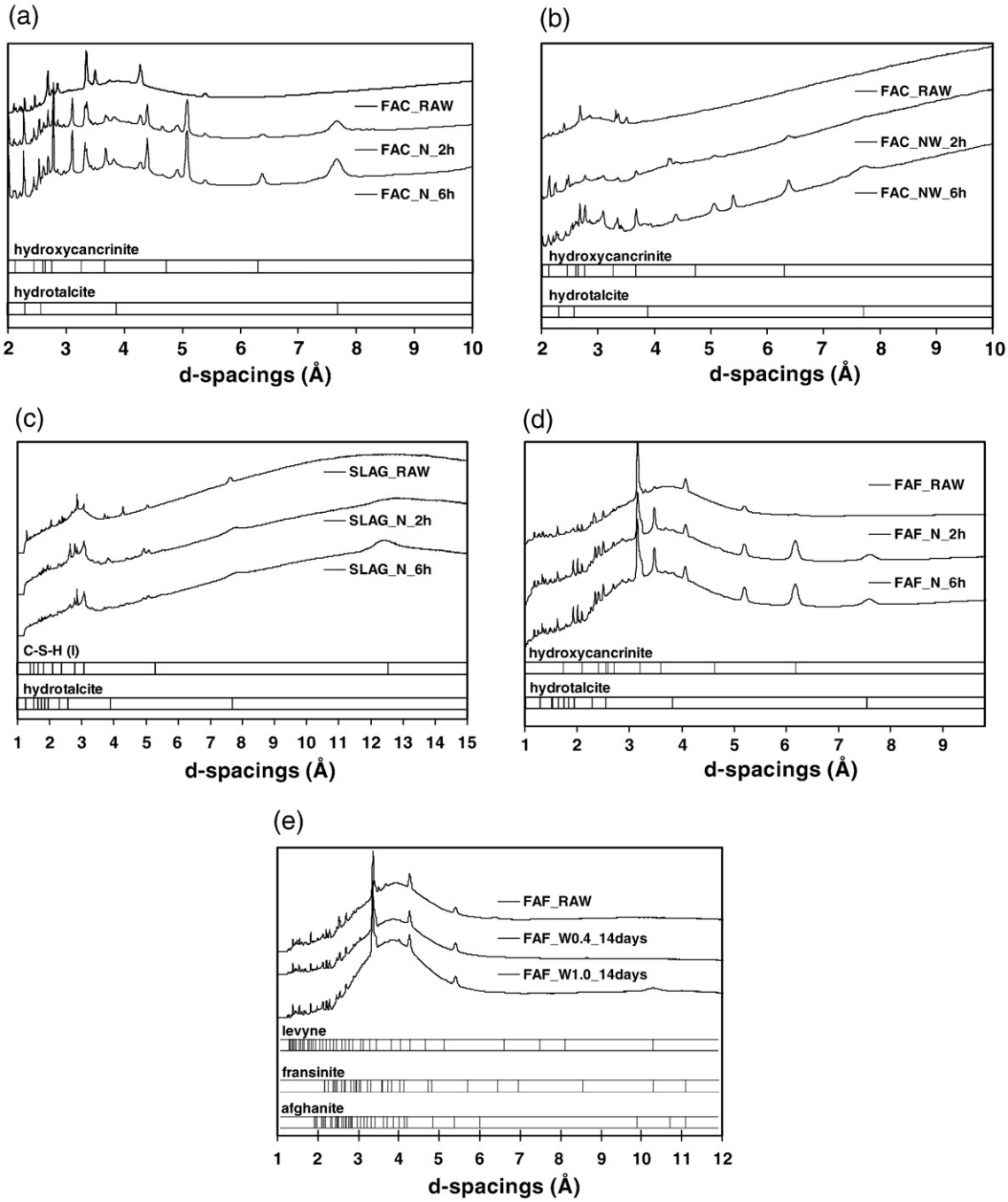

Fig. 3. XRD patterns for all samples with curing time (RAW: 0 h, 2 h: 2 h, 6 h: 6 h, and 14 days: 14 days of curing). All curing temperatures were 80 °C; (a) Class C fly ash activated with NaOH solution only (FAC_N), (b) Class C fly ash activated with mixture of NaOH and waterglass (FAC_NW), (c) slag activated with NaOH solution only (SLAG_N), (d) Class F fly ash activated with NaOH solution only (FAF_N), and (e) Class F fly ash activated with waterglass only (FAF_W). Note that XRD patterns of FAC_RAW between (a) and (b) are different in intensities due to different XRD settings but all peak positions are the same. As regards FAC_W and SLAG_W, because they have no change in the patterns, they are excluded.

3. The high calcium content in FAC seems to reduce the final mechanical strength of the cured material. The calcium in SLAG seems to increase the final mechanical strength. This is because the Ca in SLAG is available to form C-S-H (I) while it is not available in FAC. This difference must be due to the different chemical forms of calcium in these raw materials.
4. In the absence of NaOH, a high modulus of waterglass (Ms = 3.22, Ms = SiO_2/Na_2O, pH = 11.02) made the workability of the Ca-rich paste severely worse and resulted in lower strength development. It did not show any new peaks in the XRD patterns. It seems that the Ms of waterglass is important for strength development.
5. Addition of waterglass to the NaOH activator does not create any new phase in FAC geopolymer although it largely enhanced the compressive strength as well as the rate of strength development.

Acknowledgements

This publication was based on work supported in part by Award No. KUS-l1-004021, made by King Abdullah University of Science and Technology (KAUST). The Advanced Light Source is supported by the Director, Office of Science, Office of Basic Energy Sciences, of the U.S. Department of Energy under Contract No. DE-AC02-05CH11231.

Table 4
Identified newly emerged XRD reflections.

d-spacings (Å)						Identified phase (typical *d*-spacings in Å)
FAC_N	FAC_NW	FAF_N	SLAG_N	FAF_W1.0	FAF_W0.4	
–	–	–	12.50	–	–	C-S-H (I) (12.5)
–	–	–	–	11.03	–	ABC-6 family type mineral
–	–	–	–	10.30	10.30	ABC-6 family type mineral
–	–	–	–	–	8.64	ABC-6 family type mineral
–	–	–	–	8.48	–	ABC-6 family type mineral
7.73	7.69	7.74	7.77	–	–	Hydrotalcite (7.64–7.844)
7.32	7.29	–	–	–	–	
6.38	6.38	6.37	–	–	–	Hydroxycancrinite (6.30–6.43)
5.40	5.41	–	–	–	–	
5.07	5.06	5.08	5.08	–	–	
–	–	–	4.93	–	–	$Ca(OH)_2$ (4.88–4.95)
–	–	–	4.66	–	–	
4.39	4.38	–	4.40	–	–	Calcium-related phase
4.27	4.26	–	–	–	–	
–	–	–	4.23	–	–	
–	–	4.04	–	–	–	
–	–	–	–	4.00	4.00	ABC-6 family type mineral
–	3.93	–	–	–	–	
3.85	3.85	3.89	3.85	–	–	Hydrotalcite (3.82–3.914)
–	–	–	3.71	–	–	
3.68	3.68	3.67	–	–	–	Hydroxycancrinite (3.66–3.68)
–	–	–	–	3.64	–	
–	–	–	3.54	–	–	
3.34	3.34	–	–	–	–	
–	–	–	3.33	–	–	
–	–	3.19	3.19	–	–	
3.10	3.10	–	–	–	–	
3.06	3.07	–	3.07	–	–	C-S-H (I) (3.07)/hydroxycancrinite (3.06–3.07)
2.82	–	–	2.79	–	–	C-S-H (I) (2.8)
2.78	2.77	–	2.77	–	–	
–	–	–	2.74	–	–	
2.70	–	–	–	–	–	
–	–	–	2.66	–	–	
–	–	–	2.63	–	–	$Ca(OH)_2$ (2.62–2.64)
2.61	2.61	2.60	2.59	–	–	Hydrotalcite (2.566–2.608)
2.53	2.53	2.53	2.54	–	–	Hydroxycancrinite (2.531–2.534)
2.46	2.46	2.46	–	2.46	2.46	ABC-6 family type mineral
2.43	2.43	–	–	–	–	Hydroxycancrinite (2.433–2.435)
–	2.33	–	–	–	–	
2.28	2.29	2.29	2.27	–	–	Hydrotalcite (2.28–2.33)
–	2.26	–	–	–	–	
–	–	2.24	–	–	–	
2.11	–	–	–	–	–	C-S-H (I) (2.10)
–	–	–	2.06	–	–	
	–	–	–	–	2.03	ABC-6 family type mineral
2.01	2.01	–	2.02	–	–	Calcium-related phase
–	1.98	–	–	–	–	
–	–	–	1.93	–	–	$Ca(OH)_2$ (1.92–1.94)/hydrotalcite (1.94–1.96)
–	1.84	–	1.83	–	–	C-S-H (I) (1.83)
–	–	–	1.80	–	–	$Ca(OH)_2$ (1.79–1.80)
1.77	1.77	1.77	–	–	–	Hydroxycancrinite (1.762–1.766)
1.72	1.72	–	1.73	–	–	Calcium-related phase
–	–	–	1.69	–	–	$Ca(OH)_2$ (1.69)
1.66	1.66	–	1.66	–	–	C-S-H (I) (1.67)
–	–	–	1.55	–	–	$Ca(OH)_2$ (1.55–1.56)
1.46	1.46	–	–	–	–	Hydroxycancrinite (1.463–1.466)
–	–	–	1.45	–	–	$Ca(OH)_2$ (1.44–1.46)
–	–	–	1.38	–	–	
–	–	–	1.36	–	–	
–	–	–	1.28	–	–	Hydrotalcite (1.254–1.28)

C-S-H (I) phase is identified according to JCPDS 34-0002 and [32].
Hydrotalcite phase is identified according to JCPDS 14-0191, 22-0700, 41-1428 and [7].
Hydroxycancrinite is identified according to JCPDS 46-1457, 28-1036, 31-1272, and 01-088-1931.
As regards FAC_W, SLAG_W, because there was no newly emerged peak, this table does not contain the peak information.
ABC-6 family type mineral was identified based on similarities of XRD patterns of levyne (JCPDS 11-0582), franzinite (JCPDS 30-1170), SAPO-56 (JCPDS 52-1178) and afghanite (JCPDS 20-1086) with the measured peaks.

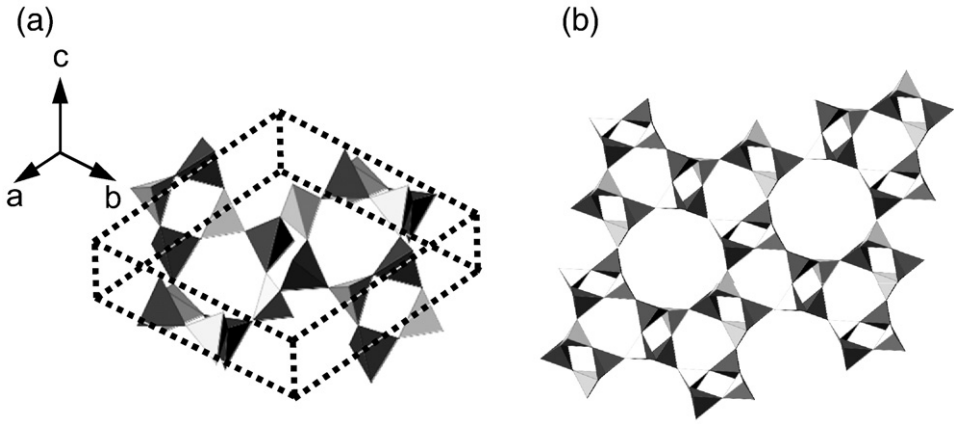

Fig. 4. Schematic drawing of basic layer of the ABC-6 family consisting of 6-membered rings. Dark gray indicates Al-tetrahedra; light gray indicates Si-based tetrahedra. (a) Dot lines imply unit cell (hexagonal, $a = 12.591$, $c = 5.117$ Å) [31]. (b) Extended drawing by connecting several unit cells shown in (a) is seen along [001].

References

[1] A. Palomo, M.W. Grutzeck, M.T. Blanco-Varela, Alkali activated fly ashes: a cement for the future, Cem. Concr. Res. 29 (1999) 1323–1329.
[2] D. Khale, R. Chaudhary, Mechanism of geopolymerization and factors influencing its development: a review, J. Mater. Sci. 42 (2007) 729–746.
[3] P. Duxson, A. Fernández-Jiménez, J.L. Provis, G.C. Lukey, A. Palomo, J.S.J. van Deventer, Geopolymer technology: the current state of the art, J. Mater. Sci. 42 (2007) 2917–2933.
[4] V.D. Glukhovsky, Soil Silicates, Gosstroy publish, Kiev (Ukraine), 1959.
[5] S. Song, H.M. Jennings, Pore solution chemistry of alkali-activated ground granulated blast-furnace slag, Cem. Concr. Res. 29 (1999) 159–170.
[6] P.J. Shilling, A. Roy, H.C. Eaton, Microstructure, strength and reaction products of ground granulated blast-furnace slag activated by highly concentrated NaOH solution, J. Mater. Res. 9 (1994) 188–197.
[7] S.D. Wang, K.L. Scrivener, Hydration products of alkali activated slag cement, Cem. Concr. Res. 25 (1995) 561–571.
[8] I.G. Richardson, A.R. Brough, G.W. Groves, C.M. Dobson, The characterization of hardened alkali-activated blast-furnace slag paste and the nature of the calcium silicate hydrate (C-S-H), Cem. Concr. Res. 24 (1994) 813–829.
[9] P. Duxon, J.L. Provis, Designing precursors for geopolymer cements, J. Am. Ceram. Soc. 91 (2008) 3864–3869.
[10] M. Criado, A. Fernandez-Jimenez, A.G. de la Torre, M.A.G. Aranda, A. Palomo, An XRD study of the effect of the SiO_2/Na_2O ratio on the alkali activation of fly ash, Cem. Concr. Res. 37 (2007) 671–679.
[11] J.L. Provis, G.C. Lukey, J.S.J. van Deventer, Do geopolymers actually contain nanocrystalline zeolites? — A reexamination of existing results, Chem. Mater. 17 (2005) 3075–3085.
[12] A. Palomo, S. Alonso, A. Fernández-Jiménez, I. Sobrados, J. Sanz, Alkaline activation of fly ashes: NMR study of the reaction products, J. Am. Ceram. Soc. 87 (2004) 1141–1145.
[13] N. Murayama, H. Yamamoto, J. Shibata, Mechanism of zeolite synthesis from coal fly ash by alkali hydrothermal reaction, Int. J. Miner. Process. 64 (2002) 1–17.
[14] G. Steenbruggen, G.G. Hollman, The synthesis of zeolites from fly ash and the properties of the zeolites products, J. Geochem. Explor. 62 (1998) 305–309.
[15] M. Inada, Y. Eguchi, N. Enomoto, J. Hojo, Synthesis of zeolite from coal fly ashes with different silica–alumina composition, Fuel 84 (2005) 299–304.
[16] X. Querol, N. Moreno, J.C. Umaña, A. Alastuey, E. Hernández, A. López-Soler, F. Plana, Synthesis of zeolites from coal fly ash: an overview, Int. Natl. J. Coal Geol. 50 (2002) 413–423.
[17] M. Kunz, A.A. MacDowell, W.A. Caldwell, D. Cambie, R.S. Celestre, E.E. Domning, R.M. Duarte, A.E. Gleason, J.M. Glossinger, N. Kelez, D.W. Plate, T. Yu, J.M. Zaug, H.A. Padmore, R. Jeanloz, A.P. Alivisatos, S.M. Clark, A beamline for high pressure studies at the Advanced Light Source with a superconducting bending magnet as the source, J. Synchrotron Radiat. 12 (2005) 650–658.
[18] A.P. Hammersley, Fit2d version 12.040, ESRF, Grenoble, France, 2006.
[19] R.W. Cheary, A.A. Coelho, Programs XFIT and FOURYA, deposited in CCP14 Powder Diffraction Library, Engineering and Physical Sciences Research Council, Daresbury Laboratory, Warrington, England, (1996) (http://www.ccp14.ac.uk/tutorial/xfit-95/xfit.htm).
[20] T. Bakharev, Geopolymeric materials prepared using class F fly ash and elevated temperature curing, Cem. Concr. Res. 35 (2005) 1224–1232.
[21] A. Fernandez-Jimenez, A. Palomo, Composition and microstructure of alkali activated fly ash binder: effect of the activator, Cem. Concr. Res. 35 (2005) 1984–1992.
[22] T. Bakharev, J.G. Sanjayan, Y.-B. Cheng, Alkali activation of Australian slag cements, Cem. Concr. Res. 29 (1999) 113–120.
[23] S.D. Wang, K.L. Scrivener, P.L. Pratt, Factors affecting the strength of alkali-activated slag, Cem. Conc. Res. 24 (1994) 1033–1043.
[24] C. Cavani, E. Trfiro, A. Vaccari, Hydrotalcite-type anionic clays: preparation, properties and applications, Catal. Today 11/2 (1991) 173–301.
[25] K. Komnitsas, D. Zaharaki, Geopolymerisation: a review and prospects for the minerals industry, Miner. Eng. 20 (2007) 1261–1277.
[26] E. Bonaccorsi, S. Merlino, Modular microporous minerals: cancrinite-davyne group and C-S-H phases, Rev. Min. Geochem. 57 (2005) 241–290.
[27] J.L. Jambor, D.A. Vanko, New mineral names, Am. Mineral. 78 (1993) 1314–1319.
[28] [28] H.V. Bekkum, E.M. Flanigen, P.A. Jacobs, J.C. Jansen, Introduction to zeolite science and practice, Studies in Surface Science and Catalysis, Ed. Elsevier Science BV 137 Amsterdam (Holland) 2001.
[29] Y. Sugano, R. Sahara, T. Murakami, T. Narushima, Y. Iguchi, C. Ouchi, Hydrothermal synthesis of zeolite A using blast furnace slag, ISI International 45 (6) (2005) 937–945.
[30] H. Xu, J.S.J. Van Deventer, The geopolymerization of alumino-silicate minerals, Int. J. Miner. Process. 59 (2000) 247–266.
[31] I. Hassan, S.M. Antao, J.B. Parise, Cancrinite: crystal structure, phase transitions, and dehydration behavior with temperature, Am. Mineral. 91 (2006) 1117–1124.
[32] L. Heller, H.F.W. Taylor, Crystallographic Data for the Calcium Silicates, HMSO, London, 1956.